Han, Shijuan; Maberly, Stephen C; Gontero, Brigitte; Xing, Zhenfei; Li, Wei; Jiang, Hongsheng; Huang, Wenmin. 2020. **Structural basis for C4 photosynthesis without Kranz anatomy in leaves of the submerged freshwater plant Ottelia alismoides.**

Original Article

Structural basis for C_4 photosynthesis without Kranz anatomy in leaves of the submerged freshwater plant *Ottelia alismoides*

Shijuan Han[1,2], Stephen C. Maberly[3], Brigitte Gontero[4], Zhenfei Xing[5], Wei Li[1,6], Hongsheng Jiang[1], Wenmin Huang[1,4,*]

[1] Key Laboratory of Aquatic Botany and Watershed Ecology, Wuhan Botanical Garden, Chinese Academy of Sciences, Wuhan 430074, China

[2] University of Chinese Academy of Sciences, Beijing 100049, China

[3] Lake Ecosystems Group, Centre for Ecology & Hydrology, Lancaster Environment Centre, Library Avenue, Bailrigg, Lancaster LA1 4AP, UK

[4] Aix Marseille Univ CNRS, BIP UMR 7281, IMM, FR 3479, 31 Chemin Joseph Aiguier, 13402 Marseille Cedex 20, France

[5] Institute of Hydrobiology, Chinese Academy of Sciences, Wuhan 430072, China

[6] Center for Plant Ecology, Core Botanical Gardens, Chinese Academy of Sciences, Wuhan 430074, China

Running title: Leaf structure in *Ottelia alismoides*

* **Correspondence:** huangwm@wbgcas.cn

ABSTRACT

• **Background and Aims** *Ottelia alismoides* (Hydrocharitaceae) is a freshwater macrophyte that, unusually, possesses three kinds of carbon dioxide-concentrating mechanisms. Here we describe its leaf anatomy and chloroplast ultrastructure, how they are altered by CO_2 concentration and may underlie C_4 photosynthesis.

• **Methods** Light and transmission electron microscopy were used to study the anatomy of mature leaves of *O. alismoides* grown at high and low CO_2 concentrations. Diel acid change and the activity of PEP carboxylase were measured to confirm that CAM activity and C_4 photosynthesis were present.

• **Key Results** When *O. alismoides* was grown at low CO_2 the leaves performed both C_4 and CAM photosynthesis whereas with high CO_2 leaves used C_4 photosynthesis. The leaf comprised an upper and lower layer of epidermal cells separated by a large air space occupying about 22% of the leaf transverse-section area, and by mesophyll cells connecting the two epidermal layers. Kranz anatomy was absent. At low CO_2, chloroplasts in the mesophyll cells were filled with starch even at the start of the photoperiod, while epidermal chloroplasts had small starch grains. The number of chloroplasts in the epidermis was greater than in the mesophyll cells. At high CO_2, the structure was unchanged but the thickness of the two epidermal layers, the air space, mesophyll and the transverse-section area of cells and air space were greater.

• **Conclusions** Leaves of *O. alismoides* have epidermal and mesophyll cells that contain chloroplasts and large air spaces but lack Kranz anatomy. The high starch content of mesophyll cells suggests they may benefit from an internal source of CO_2, for example via C_4 metabolism, and are also sites of starch storage. The air spaces may help in the recycling of decarboxylated or respired CO_2. The structural similarity of leaves from low and high CO_2 is consistent with the constitutive nature of

bicarbonate and C_4 photosynthesis. There is sufficient structural diversity within the leaf of *O. alismoides* to support dual-cell C_4 photosynthesis even though Kranz anatomy is absent.

Key words: aerenchyma, bicarbonate use, CAM, CO_2 acclimation, CO_2-concentrating mechanism (CCM), chloroplast ultrastructure, freshwater macrophyte, Hydrocharitaceae

INTRODUCTION

In their evolution from terrestrial ancestors, freshwater plants have traded-off problems of water shortage for problems of carbon-shortage (Maberly and Gontero, 2018). Carbon-shortage is mainly caused by low rates of CO_2 diffusion across boundary layers surrounding aquatic leaves (Black et al., 1981). Additionally, especially in productive lakes, generation of CO_2 concentrations below air-equilibrium and, oxygen concentrations above air-equilibrium, can together stimulate photorespiration (Maberly, 1996; Sand-Jensen et al., 2019). In response to the absence of water shortage and the presence of carbon limitation, the leaves of submerged freshwater plants have thin cuticles, lack stomata and sub-stomatal spaces and have chloroplasts in epidermal cells (Sculthorpe, 1967). Laminar leaves are generally thin with a high specific leaf area (Enríquez et al., 1996; Poorter et al., 2009) and the lamina often comprises only two or three cell layers (Maberly and Gontero, 2018). Aerenchyma is a common feature of aquatic plants (Sculthorpe, 1967) and is present in the roots, leaves and stems of most aquatic species (Silveira et al., 2016).

In addition to these structural changes, freshwater macrophytes employ a number of avoidance, exploitation and amelioration strategies to overcome carbon limitation (Klavsen et al., 2011). Amelioration strategies involve active CO_2-concentrating mechanisms (CCMs) that increase CO_2 around the primary carboxylase, ribulose-1,5-bisphosphate carboxylase/oxygenase (Rubisco). There are three known CCMs in freshwater macrophytes: of the species investigated, about half have the ability to use HCO_3^-, 8% have CAM and 4% have C_4 (Maberly and Gontero, 2017; Iversen et al., 2019). Bicarbonate is the dominant form of inorganic carbon when pH

is between about 6.3 and 10.1 and even when CO_2 becomes depleted as pH increases, bicarbonate can be present at appreciable concentrations. C_4 photosynthesis and CAM depend on temporary fixation of bicarbonate by phosphoenolpyruvate carboxylase (PEPC) to form a C_4 compound that is subsequently decarboxylated, raising the CO_2 concentration around the active site of Rubisco (Keeley, 1981; Bowes et al., 2002). The carboxylation and decarboxylation processes are separated spatially in C_4 photosynthesis and temporally in CAM. C_4 photosynthesis reduces photorespiration during the day in aquatic and terrestrial plants. In addition, CAM can reduce the loss of carbon from dark respiration and extend the duration of carbon uptake to the night (Maberly and Madsen, 2002; Pedersen et al., 2011).

Function and structure are often closely associated (Smith et al., 2012). In freshwater macrophytes, use of bicarbonate can be associated with polar leaves with high pH produced at the adaxial/upper surface and low pH at the abaxial/lower surface (Steemann Nielsen, 1947; Prins and Elzenga, 1989). Terrestrial CAM plants have large vacuoles to store the C_4 compound, often in the form of malate, accumulated during the night (Nelson and Sage, 2008; Silvera et al., 2010). Terrestrial C_4 plants, typically have a specialised 'Kranz anatomy', that comprises mesophyll cells with C_4 photosynthesis surrounding bundle sheath cells where CO_2 is concentrated and assimilated by the Calvin-Benson-Bassham cycle (Sage and Monson, 1999). In addition to different photosynthetic enzymes, these two types of cell also differ in starch content and chloroplast ultrastructure (Edwards et al., 2004) so that the initial carboxylation and the subsequent decarboxylation can be spatially separated in these two distinctive types of photosynthetic cell (Raghavendra and Sage, 2011; Sage, 2016). However, a few terrestrial plants within the dicot Amaranthaceae family, e.g. *Bienertia cycloptera*, *Bienertia sinuspersici* and *Suaeda aralocaspica* (formerly

Borszczowia aralocaspica), operate C_4 photosynthesis through the spatial separation of dimorphic chloroplasts within a single cell (Voznesenskaya et al., 2001; Voznesenskaya et al., 2002; Voznesenskaya et al., 2003; Edwards et al., 2004; Akhani et al., 2005).

C_4 photosynthesis is also present in freshwater plants from the monocot Hydrocharitaceae family: *Egeria densa*, *Ottelia alismoides* and *Ottelia acuminata* (Casati et al., 2000; Lara et al., 2002; Zhang et al., 2014), as well as in the well-studied species *Hydrilla verticillata*, where it takes place within a single cell (Bowes and Salvucci, 1989; Bowes, 2011). In *E. densa* and *H. verticillata*, C_4 photosynthesis is induced by carbon limitation whereas in *O. alismoides* it is present in mature leaves regardless of the CO_2 concentration (Zhang et al., 2014; Shao et al., 2017; Huang et al., 2018). In contrast, the CAM activity of *O. alismoides* is facultative and is induced at low CO_2 but absent at high CO_2 (Zhang et al., 2014). In addition, *O. alismoides* has a constitutive ability to use bicarbonate and is the only plant known to have three different CCMs (Zhang et al., 2014; Shao et al., 2017; Huang et al., 2018).

In terrestrial plants, elevated CO_2 concentrations can alter anatomical structure (Pritchard et al., 1999; Uprety et al., 2001). Leaves of freshwater plants grown in air and water can have very different morphologies and structure (Maberly and Gontero, 2018). However, the anatomical response of leaves of freshwater plants to different CO_2 concentrations has not been studied. Since *O. alismoides* is the only known species with three kinds of CCMs, we hypothesized that its leaf anatomy and chloroplast ultrastructure might be peculiar and reflect the integration of these three different processes and that they might be affected by CO_2 concentration.

MATERIALS AND METHODS

Plant material

On 22 March 2018, seeds of *O. alismoides* were sown in plastic pots (11 cm in diameter and 7 cm deep) containing sterile soil from nearby Donghu Lake and covered with 2 cm of sterile tap water. The chemical composition of the tap water was analyzed. The concentrations of total nitrogen (TN) and total phosphorus (TP) were determined spectrophotometrically after digestion with $K_2S_2O_8$ (Huang et al., 1999). The concentrations of Na^+, K^+, Ca^{2+} and Mg^{2+} were determined using optical emission spectrometry (ICP-OES) Optima 8000DV (Perkin Elmer, MA, USA) after addition of 200 μL HNO_3 to 10 mL tap water. The concentrations of Cl^-, SO_4^{2-} and NO_3^- were measured using Dionex ICS-5000$^+$ HPIC system (Thermo Fisher Scientific, MA, USA). The composition is shown in Supplementary Data Table S1.

The pots were placed in a plant growth chamber at 28 °C, 12/12 hours photoperiod (150 μmol photon m^{-2} s^{-1}, photosynthetically active radiation). The water level was increased as the seedlings grew to keep them submerged. When the seedlings were about 4 cm tall, the pots were placed in 1 L glass beakers in the growth chamber. After 40 days, three to five seedlings (~8 cm tall) were transplanted into another plastic pot (15 cm diameter, 12 cm deep) containing the sterile soil. These containers were placed in a 400 L tank (64 cm deep) located in a glasshouse receiving natural daylight. The tap water in the tank was changed weekly and snails were removed daily.

Response of mature *O. alismoides* leaves to different CO_2 concentrations

In August 2018, when the plants had produced many broad, oval-shaped mature leaves, one pot was placed in each of eight white plastic buckets (25 × 25 × 35 cm). These were filled with tap water and placed in the rooftop tanks, surrounded by water to keep the water temperature consistent among all the buckets, but the solution in each bucket was independent from the others. High and low CO_2 concentrations were produced using the method described in Shao et al. (2017) with four replicates of each treatment. The water in the buckets was changed twice during the 40-days acclimation. Low CO_2 (LC) was produced by allowing plant photosynthesis to deplete inorganic carbon and increase pH while high CO_2 (HC) was produced by adding a CO_2 solution to produce a set pH twice each day. In the morning (between 08:00 and 09:00) and afternoon (between 17:30 to 19:00), the water was gently stirred to thoroughly mix it and pH was measured with a pH electrode and temperature was measured with a thermometer. Alkalinity was measured every two days by Gran titration (Shao et al., 2017). On each sampling occasion, CO_2-saturated tap water was added to the HC treatment, to bring the pH to 6.8. Concentrations of CO_2 were calculated from pH, alkalinity and temperature (Maberly, 1996). In the LC treatment, the pH increased from 8.0 to over 9.8 and the CO_2 concentration varied between 0.1 and 13 μmol L^{-1} with a mean of 2.4 μmol L^{-1}. In the HC treatment, the pH varied between 6.6 and 6.9, producing CO_2 concentrations between 481 μmol L^{-1} and 1110 μmol L^{-1} with a mean of 720 μmol L^{-1}. Water temperature ranged between 25 and 35 ºC with a mean of 30 ºC. As a reference, the CO_2 concentration in equilibrium with 400 ppm atmospheric CO_2 will be about 14 μmol L^{-1} at 30 °C. Changes in CO_2 concentration in the two treatments are shown in Supplementary Data Fig. S1. After 40-days acclimation to LC and HC treatments, fully expanded mature leaves that had been produced during the

experiment and appeared to be of similar age were sampled for structure and physiology studies.

Light Microscopy and Transmission Electron Microscopy

Leaf segments (3 mm × 3 mm) sampled at 0500 and 1800 were fixed overnight in 2.5% glutaraldehyde in 0.1 M phosphate buffer (pH 7.4) at 4°C and post-fixed in 1% OsO_4 at 4°C for 2.5 h (Farnese et al., 2017). They were dehydrated using a stepwise ethanol series (30, 50, 70, 90 and 100%) and processed with a mixed solution of ethanol and acetone, then infiltrated in a mixture of acetone and epoxy resin (1: 1 for 1 h, and then 1: 2 for 8 h) and finally embedded using SPI-PON 812 at 60°C for 48 h. Semi-thin sections (1.5 μm) and ultrathin sections (72 nm) were obtained on a Leica EM UC7 ultramicrotome. Semi-thin sections were stained with methylene blue and observed using a Motic BA310 digital light microscope. Quantitative characteristics of leaf structures were measured using the Motic Images Plus 2.0 ML software. For the ultrathin sections, after staining with uranyl acetate and lead citrate, they were observed and photographed with a HT7700 transmission electron microscope (Hitachi High-Tech, Japan). Leaf chloroplasts and starch grains in electron micrograph were measured using Image J software. The distribution of chloroplasts in cells was assessed by measuring the number of chloroplasts per unit length of cell wall at different locations from the semi-thin sections under the light microscope, including the upper epidermis next to water, the upper epidermis next to air space, the upper mesophyll cells, the lower mesophyll cells, the lower epidermis next to air space and the lower epidermis next to water.

Enzyme activity measurement

Mature leaves were collected at 0500 and 1800 using the extraction and assay protocols for Rubisco and PEPC activities as described previously (Zhang et al., 2014; Shao et al., 2017; Huang et al., 2018). Enzyme activities were calculated from the rate of disappearance of NADH at 340 nm and 25°C measured with a microplate reader (Tecan M200 PRO, Austria).

CAM activity measurement

CAM activity was assessed by calculating the daily change in titratable acidity, in leaves harvested at 0500 and 1800 as previously described (Zhang et al., 2014). Briefly, to measure leaf acid content, 10 mL CO_2-free deionized water were added to the leaf samples of known fresh weight (0.2 ~ 0.5 g) and then boiled for 30 min. The acidity was titrated to pH 8.3 using 0.01 N NaOH.

Statistical analysis

SPSS 20 (SPSS Inc., Chicago, IL, USA) was used to analyze the data. An independent sample t-test was used for two groups of data with normal distribution, the Mann-Whitney U-test was used for two groups of data where the distribution was not normal and the Kruskal-Wallis test was used for three or more groups of data where the distribution was not normal. The significance level of the statistics was accepted at $P < 0.05$.

RESULTS

C_4 photosynthesis and CAM activity

The enzyme activities of PEPC and Rubisco in mature leaves under HC and LC treatments were measured to confirm that C_4 photosynthesis was present. There was no significant difference in PEPC activities between leaves collected at dusk and dawn regardless of the treatments, but the PEPC activities were significantly higher in leaves grown at a low versus a high concentration of CO_2 (Fig. 1A). Rubisco activity was significantly lower in leaves collected at dawn versus dusk, but was not affected by CO_2 concentration (Fig. 1B). The ratio of PEPC to Rubisco was between 1.6 and 4.2 (Fig. 1C) within a range typical of terrestrial C_4 plants (Zhang et al., 2014). This ratio was significantly higher at low than at high CO_2 both at dawn and dusk. At dawn, the ratio was about 2.6-fold higher in low compared to high CO_2 leaves suggesting that leaves from low CO_2 had more active C_4 photosynthesis than those from high CO_2. Leaves at low CO_2 had a marked diel change in acidity that was significantly higher (58 μequiv g^{-1} FW) than at high CO_2 concentrations (19 μequiv g^{-1} FW, Fig. 2). These results confirm that these mature *O. alismoides* leaves perform both C_4 photosynthesis and CAM when acclimated to low CO_2 and C_4 photosynthesis at high CO_2.

Effects of CO_2 concentration on leaf anatomy

Transverse sections showed that there were no major differences in basic structure and types of cell in leaves grown at high and low concentrations of CO_2 (Fig. 3).

Leaves from both treatments comprised an upper and lower layer of epidermal cells separated by a large air space and between one and three but most often two stacked mesophyll cells connecting the two epidermal layers. In transverse section, the epidermal cells varied in shape between rectangular and elliptical while the mesophyll cells were less elongated (Fig. 3B, E). Parenchymal cells containing some chloroplasts occurred around the vascular bundle, the bundle sheath, but this was not surrounded by mesophyll cells and thus Kranz anatomy was absent (Fig. 3C, F).

Leaf width was significantly greater at high (8.56 (mean) cm ± 0.50 (SD)) compared to low CO_2 concentration (5.44 cm ± 0.18), but leaf length was unaltered at ~12 cm (Table 1). Consequently, the length to width ratio was greater at low CO_2. The leaves of *O. alismoides* were thicker at high than at low CO_2 concentration (Fig. 3, Table 1). The ratio of air space area to leaf area in transverse section was 0.22 to 0.23 but was not affected significantly by CO_2 concentration (Table 1). The air spaces were bounded top and bottom by the epidermal cells and surrounded at the sides by a network of mesophyll cells and so were not connected to one another (see also Supplementary Data Fig. S2).

The epidermis and mesophyll of plants grown at high CO_2 concentration were significantly thicker and of greater cell area than in plants grown at low CO_2 concentration (Fig. 4). Furthermore, the upper epidermis was thicker than the lower epidermis, both at low and high CO_2 ($P < 0.001$), but the area was not different. The thickness and area of an air space were correspondingly greater at high CO_2 concentration.

Effects of CO_2 concentration on chloroplasts

Chloroplasts were present in epidermal and mesophyll cells (Fig. 3). Since chloroplasts can differ in cells carrying out different processes, such as in C_4 photosynthesis, we characterized chloroplast size, shape and ultrastructure in leaves grown at high and low CO_2. In leaves grown at high CO_2, the chloroplasts in epidermis and mesophyll cells were all nearly spherical with large starch grains (Fig. 5A, C, D, E), which occupied ~65 and ~80% of the chloroplast area both at dusk and dawn (Fig. 6E & F). In contrast, in leaves grown at low CO_2, epidermal chloroplasts were spindle-shaped (Fig. 5F), while the mesophyll chloroplasts were spherical (Fig. 5I) and consequently, their minor axis length was shorter (Fig. 6B). In the leaves collected at dusk, starch occupied 40% and 64% of the chloroplast area in the epidermal and the mesophyll cells, respectively (Fig. 6E). The same trend was also observed in the leaves sampled at dawn (Fig. 6F), small and large starch grains were distributed in the chloroplasts of the epidermal and mesophyll cells, respectively (Fig. 5H & J). Grana with many thylakoids were clearly visible in epidermal chloroplasts (Fig. 5B & G) whereas in mesophyll chloroplasts, the grana thylakoids were indistinct because of the high starch content.

The average area of a chloroplast was greater in leaves grown at high versus low CO_2 in both types of cell (Fig. 6C). The area of a chloroplast was greater in mesophyll than in epidermal cells for both CO_2 treatments. At high CO_2, the number of mitochondria within 1 μm around a chloroplast in mesophyll and epidermal cells was not significantly different (Fig. 6D). However, at low CO_2, the number of mitochondria around chloroplasts in mesophyll cells was significantly higher than in the epidermal cells.

The distribution of chloroplasts in epidermal and mesophyll cells was measured under different CO_2 concentrations (Fig. 7). The frequency of chloroplasts in the upper and lower epidermis was significantly greater than in the mesophyll cells. The chloroplast frequency at the cell walls next to air spaces in the lower epidermis was less than the equivalent location in the upper epidermis, at high and low CO_2. The frequency of chloroplasts at the upper epidermis next to an air space was significantly lower in leaves acclimated to low compared to high CO_2.

DISCUSSION

Adaptation to photosynthesis underwater

The presence of chloroplasts in epidermal cells is a common feature in submerged angiosperms, but rare in their terrestrial ancestors (Sculthorpe, 1967; Rascio, 2002; Maberly and Gontero, 2018). Mature leaves of *O. alismoides* have two types of photosynthetic cell, epidermal and mesophyll. In contrast, leaves from three other species of Hydrocharitaceae, *H. verticillata, E. densa* and *Elodea callitrichoides*, only have two layers of epidermal cells and no mesophyll cells (Falk and Sitte, 1963; Pendland, 1979; Hara et al., 2015). As a consequence, the leaf thickness of *O. alismoides*, especially in the leaves grown at high CO_2, at 196 μm, is much greater than the median (95 μm) for submerged leaves from a range of freshwater macrophytes (Maberly and Gontero, 2018) and greater than *E. callitrichoides* and *E. densa* estimated from published images to be about 65 μm. While Black et al. (1981) estimated that the internal resistance to diffusion of CO_2 within the relatively thin leaves of four *Potamogeton* species (48 to 63 μm) was only 3 to 4% of the total, the internal resistance in the thicker leaves of *O. alismoides* could be greater but could be

offset by the high porosity (ratio of air space to transverse sectional leaf area, 0.22 to 0.23). In *O. alismoides*, the sizes of the upper and lower epidermal cells are similar while in *H. verticillata*, the upper epidermal cells are noticeably larger than the lower cells (Pendland, 1979). In *E. callitrichoides* the transverse sectional area of the upper epidermal cells is about four-times that of the lower epidermis (Falk and Sitte, 1963), assuming the orientation in Fig. 1 in Falk and Sitte (1963) is correct since the adaxial and abaxial layers are not specifically labelled. Similarly, in *E. densa*, the transverse sectional area of the upper epidermal cells is about five-times larger than that of the lower epidermal cells (Hara et al., 2015). The functional significance of these differences is currently unknown but they could be linked to the use of bicarbonate involving different processes in upper and lower cell layers (Steemann Nielsen, 1947; Prins and Elzenga, 1989).

Well-developed aerenchyma is a common feature of aquatic plants (Jung et al., 2008). *O. alismoides* contains large air spaces between the epidermal layers while in *H. verticillata* and *E. callitrichoides*, there are numerous small intercellular spaces between the upper and lower epidermal cells that comprise a small proportion of the leaf volume (Falk and Sitte, 1963; Pendland, 1979). In many isoetids, the aerenchyma is a large proportion of the leaf volume and is continuous from the roots to the leaves, allowing sedimentary CO_2 to be taken up and fixed (Madsen et al., 2002) and oxygen to be supplied to the roots (Sand-Jensen and Prahl, 1982). Since in *O. alismoides* the air spaces are discrete (Supplementary Data Fig. S2), and so not connected to the roots, these two processes are unlikely to occur. Air spaces comprise about 22 to 23% of the transverse section leaf area in *O. alismoides*, which is within the broad range recorded for terrestrial leaves (3 - 73%, Slaton and Smith, 2002; Earles et al., 2018). In terrestrial leaves, the intercellular air spaces are connected to the atmosphere via

stomata and help to maximize the mesophyll surface area in contact with atmospheric CO_2. Aquatic plants generally lack functional stomata, so the air spaces within a leaf are not connected to the exterior. The air spaces provide buoyancy, allowing the leaves to float towards the surface where light is higher, but could also act as a reservoir of respiratory CO_2 (Wetzel et al., 1984) or photorespiratory CO_2 (Søndergaard and Wetzel, 1980) as can also occur in terrestrial C_3 plants (Busch et al., 2013). However, a calculation for low CO_2 leaves based on a one-sided specific leaf area of 100.5 cm^2 g^{-1} FW and net rates of photosynthesis at around air-equilibrium CO_2 of 2 μmol g^{-1} FW h^{-1} (Zhang et al., 2014), air space area as a proportion of leaf area of 0.23 (this study) and maximal CO_2 partial pressure in the air space of 10,000 ppm (Madsen, 1987) suggests that air-space CO_2 could only support net photosynthesis for about 5 minutes. Nevertheless, if C_4 decarboxylation occurs in the mesophyll cells, as seems possible given the relatively high chloroplast density in these cells in relation to their distance from external inorganic carbon sources, then the air spaces may serve to trap and recycle CO_2 produced by C_4 decarboxylation. This could be efficient as loss of CO_2 from the air spaces to the outside will be limited by the chloroplasts in the epidermis and the low rate of CO_2 exchange between the leaf and the bulk water as a result of transport limitation across the boundary layer. At 25 °C the air-equilibrium molar ratio of oxygen to CO_2 in water is about 28-fold less than in air, so the air spaces may also provide a means to reduce the concentration of photosynthetically produced oxygen within mesophyll and epidermal cells.

C_4 photosynthesis and absence of Kranz anatomy

In the Hydrocharitaceae, four species are known to have constitutive or facultative C_4 photosynthesis, *H. verticillata*, *E. densa*, *O. acuminata* and *O. alismoides* (Bowes et al., 2002; Lara et al., 2002; Zhang et al., 2014; Yin et al., 2017) and lack Kranz anatomy. There is evidence that *H. verticillata* has single cell C_4 photosynthesis (Bowes et al., 2002). In this respect, it is similar to single-cell terrestrial C_4 plants (Voznesenskaya et al., 2001; Voznesenskaya et al., 2002) such as *B. cycloptera* and *S. aralocaspica* where C_4 production and decarboxylation occur in different parts of a cell (Edwards et al., 2004; Edwards and Voznesenskaya, 2011; Sharpe and Offermann, 2014; von Caemmerer et al., 2014). In these terrestrial plants, C_4 decarboxylation occurs in mitochondria using NAD malic enzyme (NAD-ME). In *O. alismoides*, Zhang et al. (2014) suggested, on the basis of enzyme activity measurements, that NAD-ME is also the decarboxylating enzyme, unlike in *H. verticillata* where NADP-ME is believed to be involved (Bowes, 2011). The location of primary CO_2 fixation and decarboxylation in *O. alismoides*, and whether they take place in a single cell, is unknown. Here we show that the mesophyll cells of *O. alismoides* have a high starch content which is consistent with these cells either being the site of high rates of photosynthesis resulting from decarboxylation, producing CO_2 locally or being sites of starch storage. However, the high frequency of mitochondria around mesophyll chloroplasts in leaves acclimated to low CO_2 supports the possibility that these cells are the site of decarboxylation by the mitochondrial NAD-ME, as does the presence of chloroplasts in mesophyll cells despite their distance from external sources of inorganic carbon. In this dual-cell model, the *O. alismoides* epidermal cells would then perform the function of the terrestrial C_4 mesophyll cells by producing a C_4 product and the *O. alismoides* mesophyll cells would perform the function of the

terrestrial C_4 bundle sheath cells in decarboxylating the C_4 product. However, it is also possible that both processes could be occurring within the mesophyll cells.

Some C_4 terrestrial plants have dimorphic chloroplasts in a single cell (Voznesenskaya et al., 2001; Voznesenskaya et al., 2002; Voznesenskaya et al., 2003; Akhani et al., 2005; Sharpe and Offermann, 2014). The different forms of chloroplasts in the Kranz anatomy cells are linked to different energy requirements and fixation of carbon (Edwards et al., 2004). Dimorphic chloroplasts differing in size and ultrastructure also occur in leaves of freshwater plants. In *Cabomba caroliniana* (Cabombaceae), the chloroplasts in mesophyll cells have larger starch grains, more thylakoids per granum, and are larger than epidermal chloroplasts (Galati et al., 2015; Table 2). Species within the aquatic angiosperm family Podostemaceae also have two types of chloroplasts. Small chloroplasts with a normal grana ultrastructure and very small starch grains occur at the upper tangential walls of epidermal cells, while large chloroplasts with more thylakoids per granum and many well-developed starch grains occur at the lower tangential walls of these cells and also in mesophyll cells (Fujinami et al., 2011; Table 2). However, there is no evidence for CCMs in *C. caroliniana* (Yin et al., 2017*)*. In the Podostemaceae, although carbon isotope values range widely between -12.8 and -38.6‰ (Ziegler and Hertel, 2007) at different locations suggesting that there could be differences in discrimination resulting from C_4 photosynthesis or bicarbonate use, differences in carbon isotope signature caused by the source inorganic carbon cannot be excluded so the presence or absence of CCMs in these plants is currently unknown.

In terrestrial C_4 plants, cells or parts of cells where C_4 fixation occurs have smaller chloroplasts with less starch than chloroplasts in cells or parts of cells where

decarboxylation occurs (Table 2). Chloroplasts from the epidermal cells of *O. alismoides* are similar to those involved in C_4 fixation while chloroplasts from mesophyll cells are similar to those involved in C_4 decarboxylation, suggesting that C_4 photosynthesis in this species may involve both cell types. However, although the biochemical evidence suggests that *O. alismoides* belongs to the NAD-ME sub-type of C_4 (Zhang et al., 2014), its pattern of thylakoids per granum in epidermal compared to mesophyll cells is closer to that of terrestrial NADP-ME C_4 plants, suggesting that there is not a direct 'read-across' between C_4 photosynthesis in aquatic and terrestrial plants.

Responses to CO_2

To maximise plant productivity there is an intricate relationship between leaf structure and function (Oguchi et al., 2018). In terrestrial plants, where water can be limiting, there is an evolutionary pressure to maximise the ratio of carbon gain to water loss. Cell size and leaf thickness are dependent on environmental conditions (Zeiger, 1983; Jones, 1985; Radoglou and Jarvis, 1990). In *Liquidambar styraciflua*, *Pinus taeda*, and *Brassica juncea*, high CO_2 also has a structural effect, increasing the thickness of the upper and lower epidermis and mesophyll cell of leaves (Rogers et al., 1983; Uprety et al., 2001). Elevated CO_2 generally increases the size of terrestrial plants (Pritchard et al., 1999). We found the same here for the freshwater plant *O. alismoides*, suggesting that the increase of this resource has a universal effect on plant size.

Conclusions

O. alismoides has three CCMs that requires structural and functional coordination to operate efficiently. Unlike terrestrial plants, the anatomy of *O. alismoides* is relatively simple, and spongy and palisade tissues are absent, as they are in submerged leaves of all aquatic plants (Maberly and Gontero, 2018). The leaf comprises two types of photosynthetic cell, epidermal and mesophyll. The conceptual overview summarizing the structure of *O. alismoides* leaves acclimated to high CO_2 and low CO_2 concentrations is shown in Supplementary Data Fig. S3. Epidermal cells, containing chloroplasts, maximise uptake of external CO_2, aided by bicarbonate use, while the mesophyll cells may be sites where CO_2 is concentrated by decarboxylation. Abundant discrete air spaces provide buoyancy but may also trap (photo)-respiratory CO_2, or CO_2 produced by decarboxylation, permitting its refixation. Overall, there is sufficient structural diversity within the leaf of *O. alismoides* to support dual-cell C_4 photosynthesis even though Kranz anatomy is absent. However, further studies are needed to conclude definitively if *O. alismoides* has dual-cell C_4 with the mesophyll cells representing the site of decarboxylation. Work is underway to test this by locating key photosynthesis enzymes in the epidermal and mesophyll cells.

SUPPLEMENTARY DATA

Supplementary data consist of the following. Figure S1: Fluctuations of CO_2 concentration in high CO_2 and low CO_2 treatments during the 40-days acclimation. Figure S2: Photographs of the surface of a mature *O. alismoides* leaf from the low CO_2 treatment using a laser scanning confocal microscope. Figure S3: Conceptual overview summarizing the structure of *O. alismoides* leaves acclimated to high CO_2 and low CO_2 concentrations. Table S1: The chemical composition of the tap water used in the growth experiments.

ACKNOWLEDGEMENTS

We thank Yuan Xiao for providing the TEM service and Jun Men for assistance in the chemical analysis of water (Analysis and Testing Center, Institute of Hydrobiology, Chinese Academy of Sciences). This work was supported by the Strategic Priority Research Program of the Chinese Academy of Sciences (XDB31000000), Chinese Academy of Sciences President's International Fellowship Initiative to SCM and BG (2015VBA023, 2016VBA006), and the National Scientific Foundation of China (31860101, 31970368).

LITERATURE CITED

Akhani H, Barroca J, Koteeva N, *et al.* 2005. *Bienertia sinuspersici* (Chenopodiaceae): a new species from Southwest Asia and discovery of a third terrestrial C_4 plant without Kranz anatomy. *Systematic Botany* **30**: 290-301.

Black MA, Maberly SC, Spence DHN. 1981. Resistances to carbon dioxide fixation in four submerged freshwater macrophytes. *New Phytologist* **89**: 557-568.

Bowes G. 2011. Single-cell C_4 photosynthesis in aquatic plants. In: Raghavendra AS, Sage RF, eds. *C_4 photosynthesis and related CO_2 concentrating mechanisms*. Dordrecht: Springer, 63-80.

Bowes G, Rao SK, Estavillo GM, Reiskind JB. 2002. C_4 mechanisms in aquatic angiosperms: comparisons with terrestrial C_4 systems. *Functional Plant Biology* **29**: 379-392.

Bowes G, Salvucci ME. 1989. Plasticity in the photosynthetic carbon metabolism of submersed aquatic macrophytes. *Aquatic Botany* **34**: 233-266.

Busch FA, Sage TL, Cousins AB, Sage RF. 2013. C_3 plants enhance rates of photosynthesis by reassimilating photorespired and respired CO_2. *Plant, Cell & Environment* **36**: 200-212.

Casati P, Lara MV, Andreo CS. 2000. Induction of a C_4-like mechanism of CO_2 fixation in *Egeria densa*, a submersed aquatic species. *Plant Physiology* **123**: 1611-1621.

Earles JM, Théroux-Rancourt G, Roddy AB, Gilbert ME, McElrone AJ, Brodersen CR. 2018. Beyond porosity: 3D leaf intercellular airspace traits that impact mesophyll conductance. *Plant physiology* **178**: 148-162.

Edwards GE, Franceschi VR, Voznesenskaya EV. 2004. Single-cell C_4 photosynthesis versus the dual-cell (Kranz) paradigm. *Annual Review of Plant Biology* **55**: 173-196.

Edwards GE, Voznesenskaya EV. 2011. C_4 Photosynthesis: Kranz forms and single-cell C_4 in terrestrial plants. In: Raghavendra AS, Sage RF, eds. *C_4 photosynthesis and related CO_2 concentrating mechanisms*. Dordrecht: Springer, 29-61.

Enríquez S, Duarte CM, Sand-Jensen K, Nielsen SL. 1996. Broad-scale comparison of photosynthetic rates across phototrophic organisms. *Oecologia* **108**: 197-206.

Falk H, Sitte P. 1963. Zellfeinbau bei Plasmolyse. *Protoplasma* **57**: 290-303.

Farnese FS, Oliveira JA, Paiva EAS, *et al.* 2017. The involvement of nitric oxide in integration of plant physiological and ultrastructural adjustments in response to arsenic. *Frontiers in Plant Science* **8**: 516.

Fujinami R, Yoshihama I, Imaichi R. 2011. Dimorphic chloroplasts in the epidermis of Podostemoideae, a subfamily of the unique aquatic angiosperm family Podostemaceae. *Journal of Plant Research* **124**: 601-605.

Galati BG, Gotelli MM, Rosenfeldt S, Lattar EC, Tourn GM. 2015. Chloroplast dimorphism in leaves of *Cabomba caroliniana* (Cabombaceae). *Aquatic Botany* **121**: 46-51.

Hara T, Kobayashi E, Ohtsubo K, *et al.* 2015. Organ-level analysis of idioblast patterning in *Egeria densa* Planch. leaves. *Plos One* **10**: e0118965.

Hodge AJ, McLean JD, Mercer FV. 1955. Ultrastructure of the lamellae and grana in the chloroplasts of *Zea mays* L. *The Journal of Biophysical and Biochemical Cytology* **1**: 605-614.

Huang WM, Shao H, Zhou SN, *et al.* 2018. Different CO_2 acclimation strategies in juvenile and mature leaves of *Ottelia alismoides*. *Photosynthesis Research* **138**: 219-232.

Huang XF, Chen WM, Cai QM. 1999. *Survey, observation and analysis of lake ecology.* Beijing: Standards Press of China (in Chinese).

Iversen LL, Winkel A, Baastrup-Spohr L, *et al.* 2019. Catchment properties and the photosynthetic trait composition of freshwater plant communities. *Science* **366:** 878-881.

Jones HG. 1985. Adaptive significance of leaf development and structural responses to environment. In: Baker NR, Davies WJ, Ong CK, eds. *Control of leaf growth*. Cambridge: Cambridge University Press, 155-173.

Jung J, Lee SC, Choi H-K. 2008. Anatomical patterns of aerenchyma in aquatic and wetland plants. *Journal of Plant Biology* **51**: 428-439.

Keeley JE. 1981. *Isoetes howellii*: a submerged aquatic CAM plant? *American Journal of Botany* **68**: 420-424.

Klavsen SK, Madsen TV, Maberly SC. 2011. Crassulacean acid metabolism in the context of other carbon-concentrating mechanisms in freshwater plants: a review. *Photosynthesis Research* **109**: 269-279.

Laetsch WM. 1968. Chloroplast specialization in dicotyledons possessing the C_4-dicarboxylic acid pathway of photosynthetic CO_2 fixation. *American Journal of Botany* **55**: 875-883.

Laetsch WM, Price I. 1969. Development of the dimorphic chloroplasts of sugar cane. *American Journal of Botany* **56**: 77-87.

Lara MV, Casati P, Andreo CS. 2002. CO_2-concentrating mechanisms in *Egeria densa*, a submersed aquatic plant. *Physiologia Plantarum* **115**: 487-495.

Maberly SC. 1996. Diel, episodic and seasonal changes in pH and concentrations of inorganic carbon in a productive lake. *Freshwater Biology* **35**: 579-598.

Maberly SC, Gontero B. 2017. Ecological imperatives for aquatic CO_2-concentrating mechanisms. *Journal of Experimental Botany* **68**: 3797-3814.

Maberly SC, Gontero B. 2018. Trade-offs and synergies in the structural and functional characteristics of leaves photosynthesizing in aquatic environments. In: Adams III WW, Terashima I, eds. *The leaf: a platform for performing photosynthesis*. Cham: Springer International Publishing, 307-343.

Maberly SC, Madsen TV. 2002. Freshwater angiosperm carbon concentrating mechanisms: processes and patterns. *Functional Plant Biology* **29**: 393-405.

Madsen TV. 1987. Interactions between internal and external CO_2 pools in the photosynthesis of the aquatic CAM plants *Littorella uniflora* (L.) Aschers and *Isoetes lacustris* L. *New Phytologist* **106**: 35-50.

Madsen TV, Olesen B, Bagger J. 2002. Carbon acquisition and carbon dynamics by aquatic isoetids. *Aquatic Botany* **73**: 351-371.

Nelson EA, Sage RF. 2008. Functional constraints of CAM leaf anatomy: tight cell packing is associated with increased CAM function across a gradient of CAM expression. *Journal of Experimental Botany* **59**: 1841-1850.

Oguchi R, Onoda Y, Terashima I, Tholen D. 2018. Leaf anatomy and function. In: Adams III WW, Terashima I, eds. *The leaf: a platform for performing photosynthesis*. Cham: Springer International Publishing, 97-139.

Pedersen O, Rich SM, Pulido C, Cawthray GR, Colmer TD. 2011. Crassulacean acid metabolism enhances underwater photosynthesis and diminishes photorespiration in the aquatic plant *Isoetes australis*. *New Phytologist* **190**: 332-339.

Pendland J. 1979. Ultrastructural characteristics of *Hydrilla* leaf tissue. *Tissue & Cell* **11**: 79-88.

Poorter H, Niinemets Ü, Poorter L, Wright IJ, Villar R. 2009. Causes and consequences of variation in leaf mass per area (LMA): a meta-analysis. *New phytologist* **182**: 565-588.

Prins HBA, Elzenga JTM. 1989. Bicarbonate utilization: function and mechanism. *Aquatic Botany* **34**: 59-83.

Pritchard SG, Rogers HH, Prior SA, Peterson CM. 1999. Elevated CO_2 and plant structure: a review. *Global Change Biology* **5**: 807-837.

P'yankov VI, Voznesenskaya EV, Kondratschuk AV, Black Jr CC. 1997. A comparative anatomical and biochemical analysis in *Salsola* (Chenopodiaceae) species with and without a Kranz type leaf anatomy: a possible reversion of C_4 to C_3 photosynthesis. *American Journal of Botany* **84**: 597-606.

Radoglou KM, Jarvis PG. 1990. Effects of CO_2 enrichment on four poplar clones. I. Growth and leaf anatomy. *Annals of Botany* **65**: 617-626.

Raghavendra AS, Sage RF. 2011. Introduction. In: Raghavendra AS, Sage RF, eds. *C_4 photosynthesis and related CO_2 concentrating mechanisms*. Dordrecht: Springer, 17-25.

Rascio N. 2002. The underwater life of secondarily aquatic plants: some problems and solutions. *Critical Reviews in Plant Sciences* **21**: 401-427.

Rogers HH, Thomas JF, Bingham GE. 1983. Response of agronomic and forest species to elevated atmospheric carbon dioxide. *Science* **220**: 428-429.

Sage RF. 2016. A portrait of the C_4 photosynthetic family on the 50th anniversary of its discovery: species number, evolutionary lineages, and hall of fame. *Journal of Experimental Botany* **67**: 4039-4056.

Sage RF, Monson RK. 1999. *C_4 plant biology.* San Diego: Academic Press.

Sand-Jensen K, Andersen MR, Martinsen KT, Borum J, Kristensen E, Kragh T. 2019. Shallow plant-dominated lakes-extreme environmental variability, carbon cycling and ecological species challenges. *Annals of Botany* **124**: 355-366.

Sand-Jensen K, Prahl C. 1982. Oxygen exchange with the lacunae and across leaves and roots of the submerged vascular macrophyte, *Lobelia dortmanna* L. *New Phytologist* **91**: 103-120.

Sculthorpe CD. 1967. *The biology of aquatic vascular plants.* London: Edward Arnold.

Shao H, Gontero B, Maberly SC*, et al.* 2017. Responses of *Ottelia alismoides*, an aquatic plant with three CCMs, to variable CO_2 and light. *Journal of Experimental Botany* **68**: 3985-3995.

Sharpe RM, Offermann S. 2014. One decade after the discovery of single-cell C_4 species in terrestrial plants: what did we learn about the minimal requirements of C_4 photosynthesis? *Photosynthesis Research* **119**: 169-180.

Silveira MJ, Harthman VC, Michelan TS, Souza LA. 2016. Anatomical development of roots of native and non-native submerged aquatic macrophytes in different sediment types. *Aquatic Botany* **133**: 24-27.

Silvera K, Neubig KM, Whitten WM, Williams NH, Winter K, Cushman JC. 2010. Evolution along the crassulacean acid metabolism continuum. *Functional Plant Biology* **37**: 995-1010.

Slaton MR, Smith WK. 2002. Mesophyll architecture and cell exposure to intercellular air space in alpine, desert, and forest species. *International Journal of Plant Sciences* **163**: 937-948.

Smith RA, Lewis JD, Ghannoum O, Tissue DT. 2012. Leaf structural responses to pre-industrial, current and elevated atmospheric [CO_2] and temperature affect leaf function in *Eucalyptus sideroxylon*. *Functional Plant Biology* **39**: 285-296.

Søndergaard M, Wetzel RG. 1980. Photorespiration and internal recycling of CO_2 in the submersed angiosperm *Scirpus subterminalis*. *Canadian Journal of Botany* **58**: 591-598.

Steemann Nielsen E. 1947. Photosynthesis of aquatic plants with special reference to the carbon-sources. *Dansk Botanisk Arkiv* **12**: 1-71.

Uprety DC, Dwivedi N, Mohan R, Paswan G. 2001. Effect of elevated CO_2 concentration on leaf structure of *Brassica Juncea* under water stress. *Biologia Plantarum* **44**: 149-152.

von Caemmerer S, Edwards GE, Koteyeva N, Cousins AB. 2014. Single cell C_4 photosynthesis in aquatic and terrestrial plants: a gas exchange perspective. *Aquatic Botany* **118**: 71-80.

Voznesenskaya EV, Edwards GE, Kiirats O, Artyusheva EG, Franceschi VR. 2003. Development of biochemical specialization and organelle partitioning in the single-cell C_4 system in leaves of *Borszczowia aralocaspica* (Chenopodiaceae). *American Journal of Botany* **90**: 1669-1680.

Voznesenskaya EV, Franceschi VR, Kiirats O, Artyusheva EG, Freitag H, Edwards GE. 2002. Proof of C_4 photosynthesis without Kranz anatomy in *Bienertia cycloptera* (Chenopodiaceae). *The Plant Journal* **31**: 649-662.

Voznesenskaya EV, Franceschi VR, Kiirats O, Freitag H, Edwards GE. 2001. Kranz anatomy is not essential for terrestrial C_4 plant photosynthesis. *Nature* **414**: 543-546.

Wetzel RG, Brammer ES, Forsberg C. 1984. Photosynthesis of submersed macrophytes in acidified lakes. I. Carbon fluxes and recycling of CO_2 in *Juncus bulbosus* L. *Aquatic Botany* **19**: 329-342.

Woo KC, Anderson JM, Boardman NK, Downton WJS, Osmond CB, Thorne SW. 1970. Deficient photosystem II in agranal bundle sheath chloroplasts of C_4 plants. *Proceedings of the National Academy of Sciences* **67**: 18-25.

Yin L, Li W, Madsen TV, Maberly SC, Bowes G. 2017. Photosynthetic inorganic carbon acquisition in 30 freshwater macrophytes. *Aquatic Botany* **140**: 48-54.

Zeiger E. 1983. The biology of stomatal guard cells. *Annual Review of Plant Physiology* **34**: 441-475.

Zhang Y, Yin L, Jiang H-S, Li W, Gontero B, Maberly SC. 2014. Biochemical and biophysical CO_2 concentrating mechanisms in two species of freshwater macrophyte within the genus *Ottelia* (Hydrocharitaceae). *Photosynthesis Research* **121**: 285-297.

Ziegler H, Hertel H. 2007. Carbon isotope fractionation in species of the torrenticolous families Podostemaceae and Hydrostachyaceae. *Flora* **202**: 647-652.

Legends

FIG. 1. Influence of CO_2 concentration on activities of enzymes from *O. alismoides* leaves collected at dusk (1800) and dawn (0500). (A) PEPC activity. (B) Rubisco activity. (C) Ratio of PEPC to Rubisco activity. The mean values (n = 3-4), with their SD are shown. The statistical differences between means were tested using independent sample t-tests in panel A and B and independent sample t-tests and the Mann-Whitney U test in panel C. The statistic above the horizontal line compares leaves exposed to high CO_2 (black bars) and low CO_2 (white bars) collected at the same time (*NS* not significant, $^{*}P < 0.05$, $^{***}P < 0.001$); data with different small and large letters are significantly different between dusk and dawn, under high and low CO_2 treatments respectively ($P < 0.05$).

FIG. 2. Influence of high CO_2 (HC) and low CO_2 (LC) on acidity of *O. alismoides* leaves from dusk (1800) and dawn (0500). The mean values (n = 3-4), with their SD are shown. The statistical differences between means were tested using independent sample t-tests and the Mann-Whitney U test. The statistic above the horizontal line compares acidity in dusk and dawn (*NS* not significant, $^{**}P < 0.01$) within the same CO_2 treatment; changes in acidity with different letters are significantly different between HC and LC treatments ($P < 0.05$).

FIG. 3. Transverse sections of *O. alismoides* leaves under high CO_2 concentration (A-C) and low CO_2 concentration (D-F) at dusk (1800). a, air space; le, lower epidermis; m, mesophyll cell; ue, upper epidermis; v, vascular bundle. The arrowhead indicates the chloroplasts. Scale bar = 100 μm.

FIG. 4. Effects of CO_2 concentration on anatomical characteristics of *O. alismoides* leaves. (A) The thickness of upper epidermis, lower epidermis, mesophyll and air space in transverse section. (B) The area of upper epidermal cell, lower epidermal cell, mesophyll cell and air space in transverse section. The mean values ($n \geq 30$), with their SD are shown. The statistical differences between means were tested using independent sample t-tests and the Mann-Whitney U test. The statistic above the

horizontal line compares leaves under high CO_2 (black bars) and low CO_2 (white bars) concentration ($^{*}P < 0.05$, $^{**}P < 0.01$, $^{***}P < 0.001$).

FIG. 5. Ultrastructure of chloroplasts in *O. alismoides* leaves under different CO_2 concentrations and times of day. The upper row cells are from high and the lower row cells from low CO_2 concentration. A, B, F and G are epidermal cells at dusk (1800). C and H are epidermal cells at dawn (0500). D and I are mesophyll cells from dusk (1800) and E and J are mesophyll cells from dawn (0500). cw, cell wall; g, grana; m, mitochondria; p, plastoglobuli; s, starch grain. Scale bar = 1 μm.

FIG. 6. Effects of CO_2 concentration on characteristics of chloroplasts located in epidermal and mesophyll cells of *O. alismoides* leaves. (A & B) Chloroplast major and minor axis length at dusk (1800). (C) Area of chloroplast at dusk (1800). (D) Number of mitochondria within 1 μm of a chloroplast at dusk (1800). (E & F) Area ratio of starch to chloroplast in *O. alismoides* leaves collected at dusk (1800) and dawn (0500). The mean values ($n \geq 20$), with their SD are shown. The statistical differences between means were tested using independent sample t-tests in panels A and C and independent sample t-tests and the Mann-Whitney U test in panels B, D, E and F. The statistic above the horizontal line compares high CO_2 (black bars) with low CO_2 (white bars) treatments (*NS* not significant, $^{*}P < 0.05$, $^{**}P < 0.01$, $^{***}P < 0.001$); data with different small and large letters are significantly different between chloroplasts in the two cell types, under high and low CO_2 treatments respectively ($P < 0.05$).

FIG. 7. The number of chloroplasts per unit length of cell wall under different CO_2 concentrations at dusk (1800). UEW, Upper epidermis, wall next to water; UEA, Upper epidermis, wall next to air space; UM, Upper mesophyll cell; LM, Lower mesophyll cell; LEA, Lower epidermis, wall next to air space; LEW, Lower epidermis, wall next to water. Error bars represent SD ($n \geq 20$). The statistic above the horizontal line compares high CO_2 (black bars) and low CO_2 (white bars) treatments based on independent sample t-tests and the Mann-Whitney U-test (*NS* not significant,

$^{**}P < 0.01$); data with different small and large letters are significantly different among different locations based on the Kruskal-Wallis test ($P < 0.05$) under high and low CO_2 treatments.

SUPPLEMENTARY INFORMATION

Supplementary Data Fig. S1. Fluctuations of CO_2 concentration in high CO_2 and low CO_2 treatments during the 40-days acclimation.

Supplementary Data Fig. S2. Photographs of the surface of a mature *O. alismoides* leaf from the low CO_2 treatment using a laser scanning confocal microscope.

Supplementary Data Fig. S3. Conceptual overview summarizing the structure of *O. alismoides* leaves acclimated to high CO_2 and low CO_2 concentrations.

Supplementary Data Table S1. The chemical composition of the tap water used in the growth experiments.

Table 1. Influence of CO_2 concentration on characteristics of *O. alismoides* leaves. The mean values are given with SD in parenthesis. Significant differences between leaves treated with different CO_2 concentration are shown based on independent sample t-test (*NS* not significant, $^{*}P < 0.05$, $^{***}P < 0.001$).

Characteristics	High CO_2	Low CO_2	Significance	n
Leaf length (cm)	12.08 (0.36)	11.58 (0.68)	NS	5
Leaf width (cm)	8.56 (0.50)	5.44 (0.18)	***	5
Length-width ratio	1.41 (0.06)	2.13 (0.12)	***	5
Leaf thickness (μm)	196 (17)	161 (18)	*	4
The ratio of air space to leaf area in transverse section	0.22 (0.03)	0.23 (0.02)	NS	4

Table 2. Characteristics of dimorphic chloroplasts in aquatic and terrestrial plants.

Environment /type/ species	Location	Area (μm^2)	Thylakoids per granum	Starch	References
Aquatic C_3					
Hydrobryum khaoyaiense	E	3.7 ± 1.8	3~4	+	Fujinami et al. (2011)
	E	23.7 ± 11	4~5	+ + +	
Cabomba caroliniana	E	~3.8[a]	~9	+	Galati et al. (2015)
	M	~33.2[a]	~29	+ +	
Aquatic NAD-ME C_4					
Ottelia alismoides[b]	E	9.0 ± 2.3	+ +	+ +	This study
	M	13.8 ± 3.3	+	+ + +	
Terrestrial NADP-ME C_4					
Zea mays	M	Small	+ + +	+ +	Hodge et al. (1955); Laetsch (1968)
	BS	Large	+	+ + +	
Saccharum officinarum	M	Small	+ + +	+	Laetsch and Price (1969)
	BS	Large	–	+ + +	
Sorghum bicolor	M	nd	+ + +	nd	Woo et al. (1970)
	BS	nd	–	nd	
Salsola australis	M	6.67~8.2[a]	6~12	+	P'yankov et al. (1997)
	BS	14.6~16.1[a]	2~5	+ + +	
Terrestrial NAD-ME C_4					
Amaranthus edulis	P	Small	+ +	+	Laetsch (1968)
	BS	Large	+ +	+ + +	
Atriplex lentiformis	P	nd	2~3	+	Laetsch (1968)
	BS	nd	+ +	+ + +	
Atriplex spongiosa	M	nd	+	nd	Woo et al. (1970)
	BS	nd	+ + +	nd	
Terrestrial Single-cell NAD-ME C_4					
Bienertia cycloptera	C[c]	nd	~ 2	–	Voznesenskaya et al. (2002)
	C[d]	nd	3~5	+ +	
Suaeda aralocaspica	C[c]	3.48~4.0[a]	+	+	Voznesenskaya et al. (2003)
	C[d]	7.18~8.0[a]	+ + +	+ + +	

[a] Calculated according to axis length in reference
[b] Plants treated with low CO_2 concentrations
[c] Chloroplasts have structural characteristics like those in mesophyll
[d] Chloroplasts have structural characteristics like those in bundle sheath cell
– Lack grana/starch; + Rudimentary grana/starch; + + Contain grana/starch; + + + Well-developed grana/starch; BS = Bundle sheath cell; C = Chlorenchyma cell; E = Epidermal cell; M = Mesophyll cell; P = Palisade cell; nd = not determined.

Fig. 1

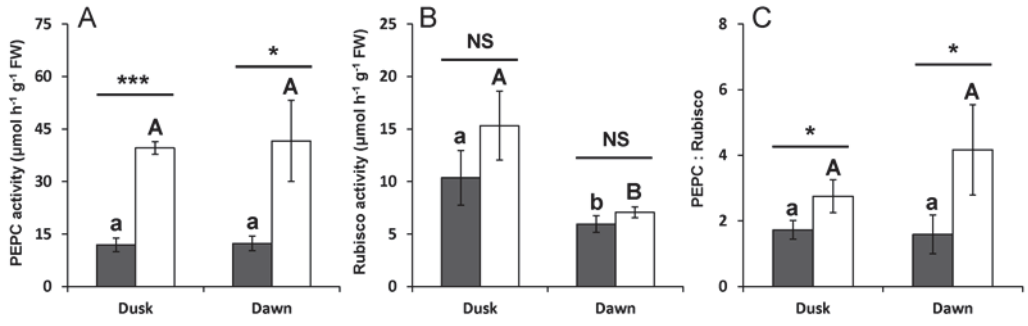
A
PEPC activity (µmol h-1 g-1 FW)
75
60
45
30
15
0
***
*
a
A
a
A
Dusk
Dawn
B
Rubisco activity (µmol h-1 g-1 FW)
25
20
15
10
5
0
NS
NS
a
A
b
B
Dusk
Dawn
C
PEPC : Rubisco
8
6
4
2
0
*
*
a
A
a
A
Dusk
Dawn

1

2

1

Fig. 2

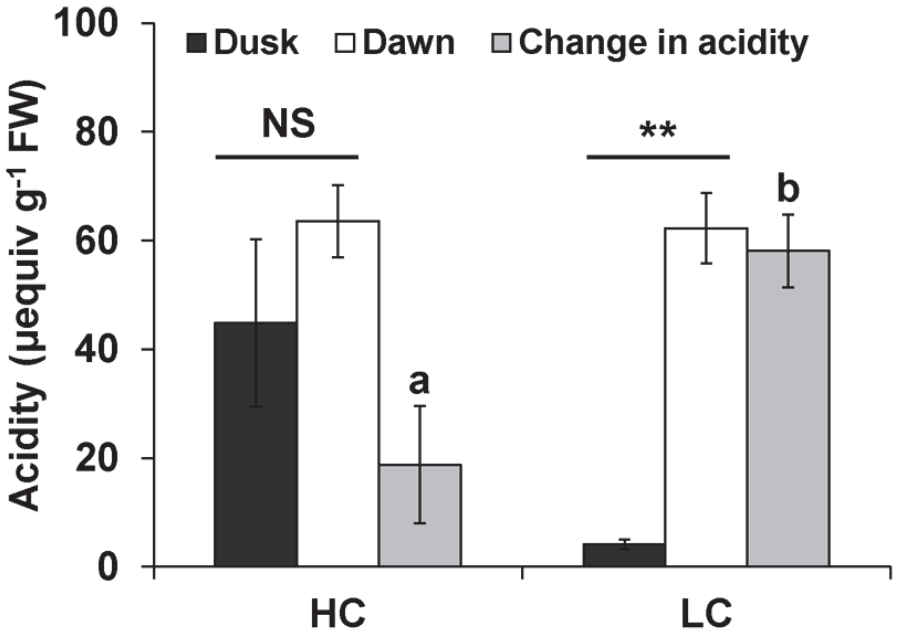
Dusk
Dawn
Change in acidity
Acidity (µequiv g-1 FW)
100
80
60
40
20
0
NS
**
a
b
HC
LC

2

3

1

Fig. 3

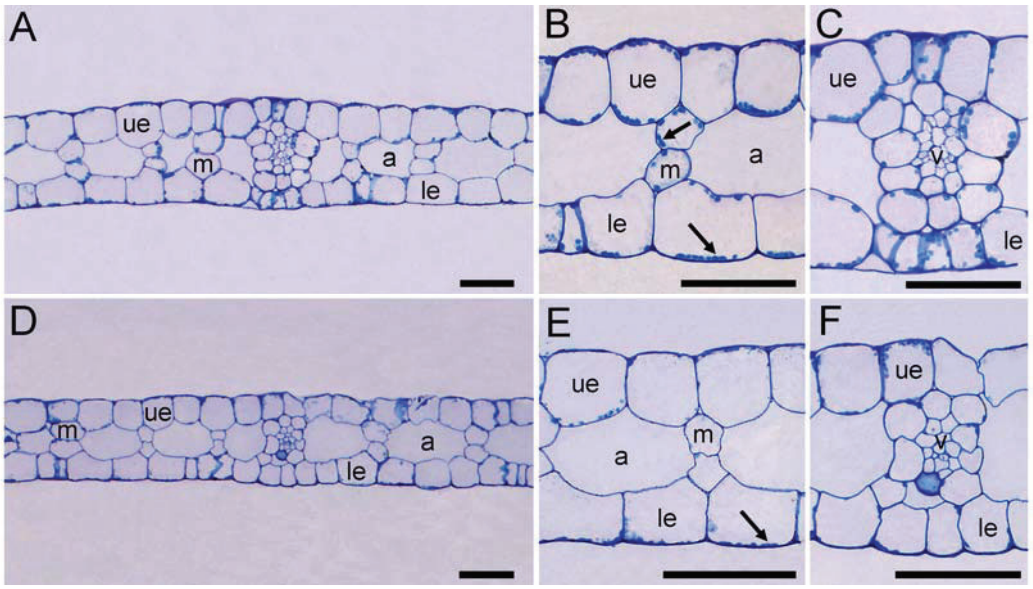

2

3

1

Fig. 4

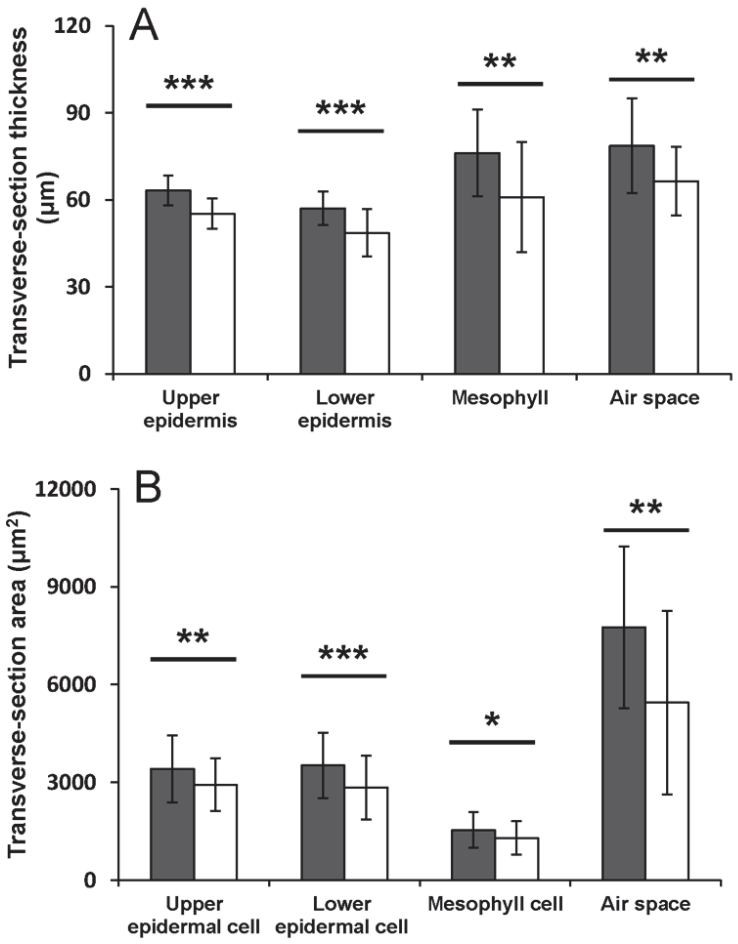
A
Transverse-section thickness (μm)
120
90
60
30
0
***
***
**
**
Upper epidermis
Lower epidermis
Mesophyll
Air space
B
Transverse-section area (μm²)
12000
9000
6000
3000
0
**
***
*
**
Upper epidermal cell
Lower epidermal cell
Mesophyll cell
Air space

2

3

Fig. 5

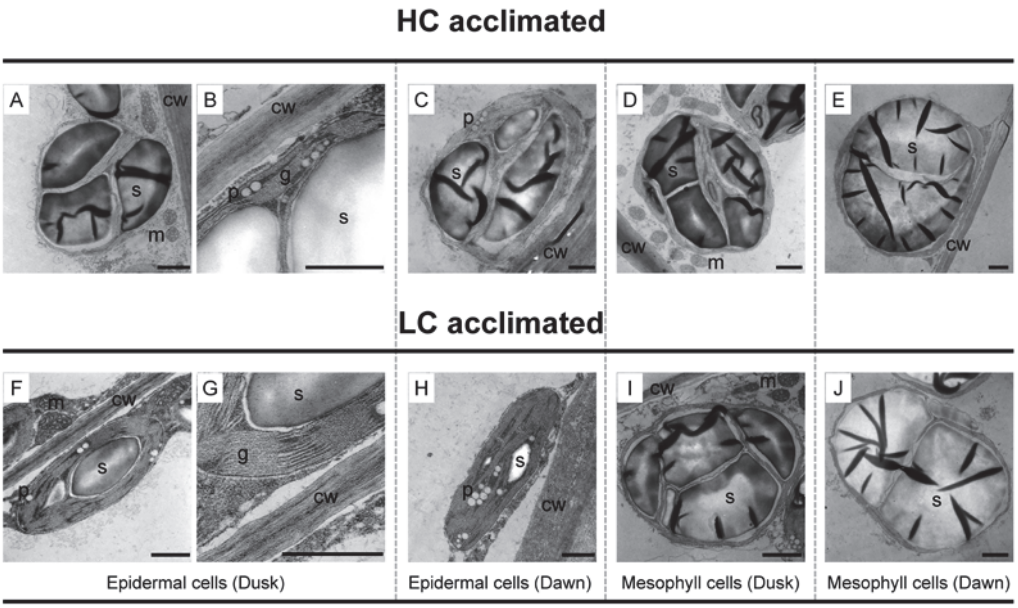
HC acclimated
A
cw
s
m
B
cw
p
g
s
C
p
s
cw
D
s
cw
m
E
s
cw
LC acclimated
F
m
cw
s
p
G
s
g
cw
H
s
p
cw
I
cw
m
s
J
s
Epidermal cells (Dusk)
Epidermal cells (Dawn)
Mesophyll cells (Dusk)
Mesophyll cells (Dawn)

1

Fig. 6

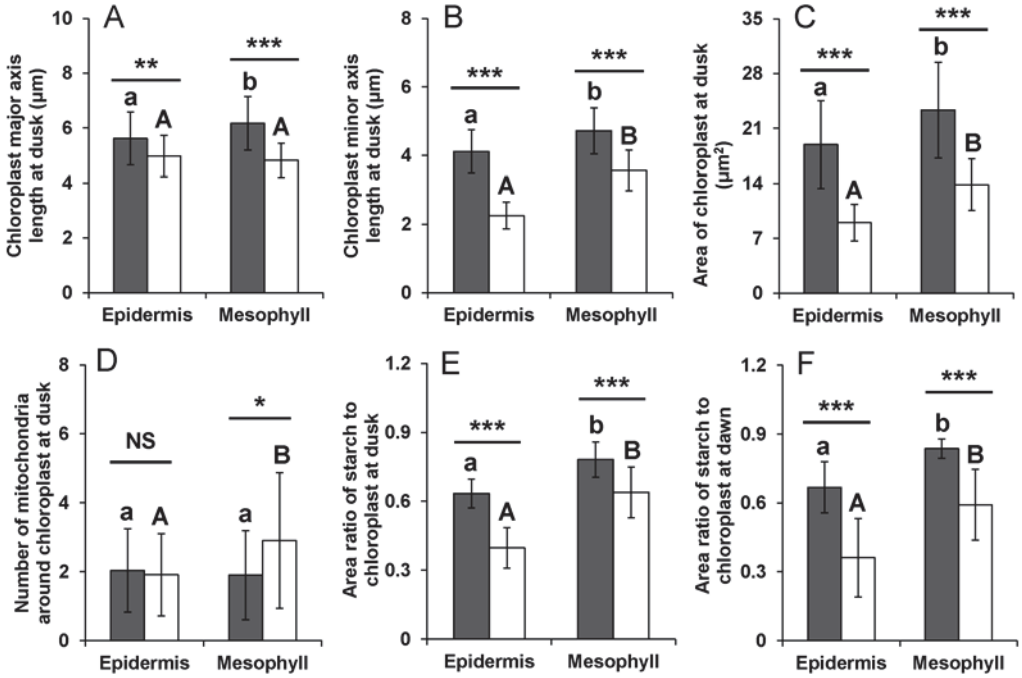
A
Chloroplast major axis length at dusk (µm)
10
8
6
4
2
0
**
***
a
A
b
A
Epidermis
Mesophyll
B
Chloroplast minor axis length at dusk (µm)
8
6
4
2
0
***
***
a
A
b
B
Epidermis
Mesophyll
C
Area of chloroplast at dusk (µm²)
35
28
21
14
7
0
***
***
a
A
b
B
Epidermis
Mesophyll
D
Number of mitochondria around chloroplast at dusk
8
6
4
2
0
NS
*
a
A
a
B
Epidermis
Mesophyll
E
Area ratio of starch to chloroplast at dusk
1.2
0.9
0.6
0.3
0
***
***
a
A
b
B
Epidermis
Mesophyll
F
Area ratio of starch to chloroplast at dawn
1.2
0.9
0.6
0.3
0
***
***
a
A
b
B
Epidermis
Mesophyll

2

3

1

Fig. 7

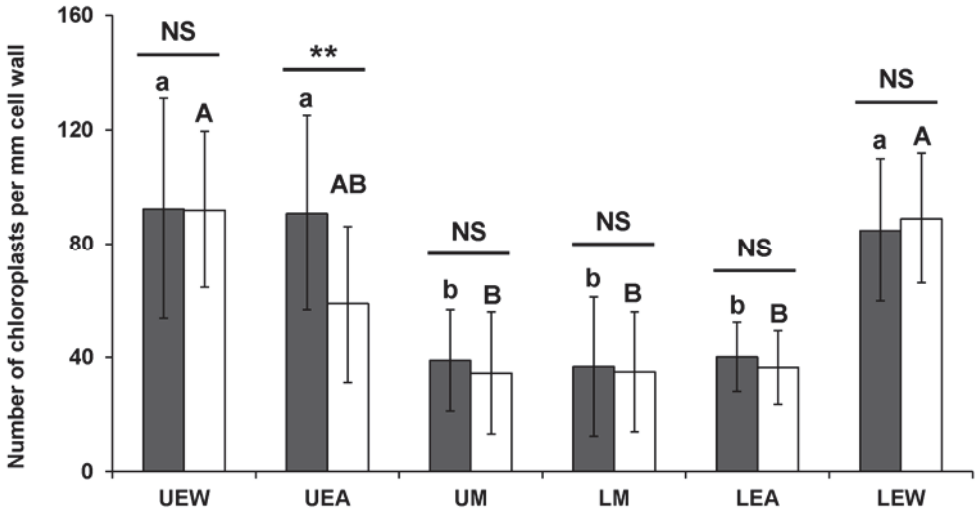
Number of chloroplasts per mm cell wall
160
120
80
40
0
NS
**
NS
NS
NS
NS
a
A
a
AB
b
B
b
B
b
B
a
A
UEW
UEA
UM
LM
LEA
LEW

2

3

1

Fig. S1

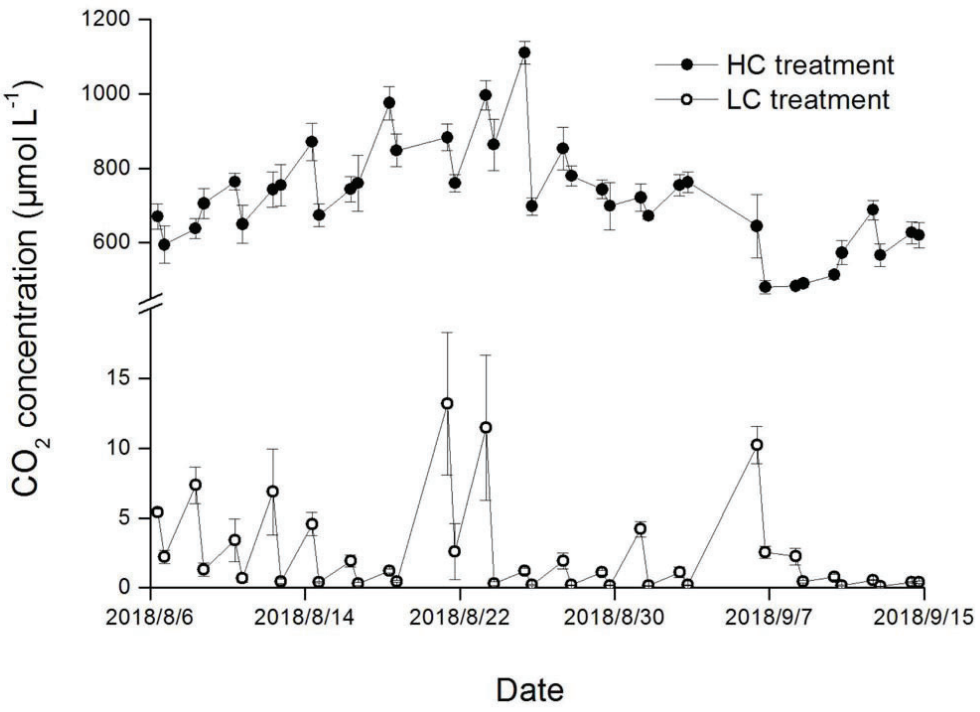
HC treatment
LC treatment
CO_2 concentration (μmol L^{-1})
1200
1000
800
600
15
10
5
0
2018/8/6
2018/8/14
2018/8/22
2018/8/30
2018/9/7
2018/9/15
Date

2

3

Fig. S2

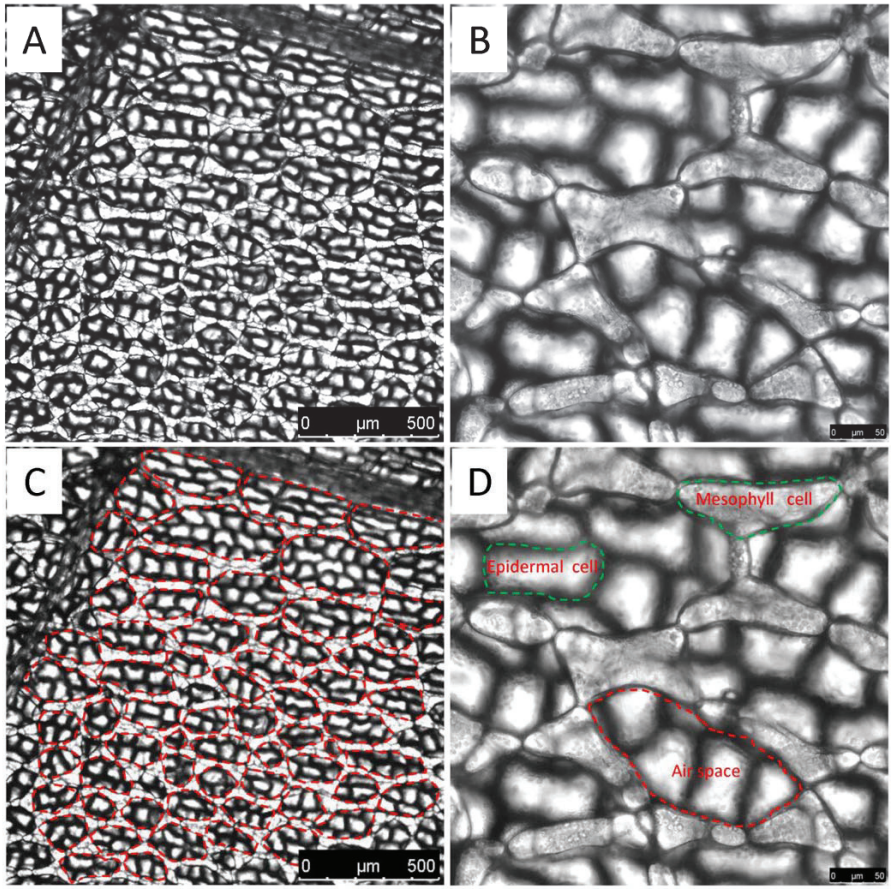
A
0 µm 500
B
C
0 µm 500
D
Mesophyll cell
Epidermal cell
Air space

Fig. S3

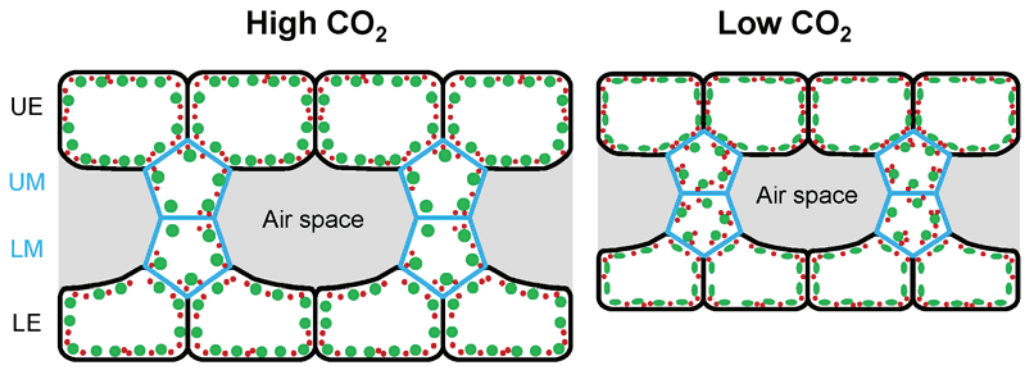

1 Table S1

2

Component	Mean (SD)
Alkalinity	2200 (10)
TP	1.61 (0.32)
TN	100 (5)
Na^+	635 (15)
K^+	130 (19)
Ca^{2+}	2255 (21)
Mg^{2+}	789 (6)
Cl^-	590 (2)
SO_4^{2-}	670 (3)
NO_3^-	86 (2)

3